Electron spin splitting in polarization-doped group-III nitrides

V. I. Litvinov*
WaveBand Corporation, 17152 Armstrong Ave., Irvine, California 92614, USA

(Received 15 May 2003; revised manuscript received 23 July 2003; published 16 October 2003)

The Rashba spin-orbit splitting parameter has been calculated in wurtzite GaN/AlGaN heterostructures. Despite the fact that wide-bandgap semiconductors are expected to have a smaller spin-orbit coupling parameter than that in InGaAs-based III-V materials, the electron spin-split energy in GaN/AlGaN heterostructure is predicted to have the same order of magnitude, due to the strong polarization field at the interface and polarization-induced doping. This, taken together with the existence of room-temperature ferromagnetism in GaN(Mn), could make the GaN-based material system competitive in spintronic applications.

DOI: 10.1103/PhysRevB.68.155314 PACS number(s): 73.40.Kp, 71.70.Ej, 77.65.Bn

I. INTRODUCTION

Heterostructures and quantum wells (QW's) based on GaAs, InAs, GaSb, and InP materials are recognized as a platform for semiconductor spintronic devices as they provide additional spin transport functionality to electronic and optoelectronic devices. The electrically controlled spin transport, relatively large spin dephasing time (≈ 100 ns, $T = 5$ K),[1,2] and ferromagnetism in GaAs(Mn) ($T_c \approx 110-140$ K)[3–5] make these materials attractive for semiconductor spintronics. Gate-controlled electron spin splitting near interfaces in narrow-gap III-V nanostructures is at the origin of spintronic proposals such as spin transistors[6,7] and quantum computers.[8]

In crystals with inversion asymmetry of the crystal potential, the spin-orbit interaction lifts the spin degeneracy of electrons and holes. The magnitude of spin splitting depends on an electron wave vector **k**. Inversion asymmetry in bulk zinc blende crystals results in k^3-dependent spin splitting (Dresselhaus terms),[9,10] whereas the structural inversion asymmetry near a heterointerface leads to an additional k-linear contribution $\pm 2\alpha k_{\parallel}$ (Rashba term),[11] where $k_{\parallel}$, α, are the in-plane wave vector and spin-orbit coupling parameter, respectively. Coupling parameter α in group III-V cubic materials was calculated first using a two-band model spectrum[12] and then using a more realistic multiband Kane model.[13–17] Typical values of α in InAs/GaSb, InP/InGaAs, and InAs/InGaAs QW's are $(0.6-4)10^{-11}$ eV m, which gives an electron spin-splitting energy of the order of (1–10) meV depending on the doping level.[18]

Search for spintronic semiconductors is ongoing as all-semiconductor devices are expected to provide effective spin injection into an active region of the device. Lack of room-temperature (RT) ferromagnetic semiconductors lattice matched to the InGaAs and InP materials makes it difficult to find the proper material combination that provides high-spin-injection efficiency. In this respect, the wide bandgap materials might have been useful since RT ferromagnetism has been projected in magnetically doped group-III nitrides theoretically[19,20] and found experimentally.[21–23] It is known, however, that the spin-orbit coupling parameter α decreases as a bandgap increases. Thus in larger bandgap materials, comparable spin splitting is not expected. Fortunately, the spin splitting, being approximately proportional to an average electric field in the growth direction, could be affected and engineered by a polarization field near an interface in the group-III-nitride heterostructure. It is known that a lattice polarization strongly affects the performance of GaN-based electronic and optoelectronic devices.[24–30] In addition, the spin splitting depends not only on α, it also increases with the carrier density. Strong polarization doping effect in group-III nitrides may compensate to some extent for the smallness of the coupling parameter and make overall spin-splitting comparable to that found in narrow-gap group-III-V structures. This fact, accompanied with the existence of RT ferromagnetism, could make group-III-nitride structures competitive in emerging spintronics applications.

The purpose of this paper is to explore some spintronic capabilities of wurtzite group-III-nitride heterostructures and QW, namely, to calculate the spin-orbit coupling parameter, conduction-band spin splitting, and its sensitivity to a gate voltage. The role the polarization field plays in spin splitting of confined electrons is discussed. General expressions for the coupling parameter are obtained for GaN/AlGaN heterostructures and QW. Numerical calculations are performed for a high-electron-mobility transistor (HEMT) structure, where the polarization-induced doping results in a high density of two-dimensional (2D) electrons. Calculations for an asymmetric QW will be done elsewhere.

II. HAMILTONIAN AND BASIC EQUATIONS

We start with a 8×8 Hamiltonian which includes conduction and valence bands[31,32]

$$H=\frac{p^2}{2m_0}+H_{8\times 8}. \tag{1}$$

The nonzero matrix elements are given as

$$H_{11}=H_{55}=E_C,\ \ H_{22}=H_{66}=F,\ \ H_{33}=H_{77}=G,$$

$$H_{44}=H_{88}=\lambda,\ \ H_{38}=H_{47}=\sqrt{2}\Delta_3,$$

$$H_{12}=H_{57}=-\frac{P_2k_+}{\sqrt{2}},\ \ H_{13}=H_{56}=\frac{P_2k_-}{\sqrt{2}},$$

$$H_{14}=H_{58}=P_1k_z, \tag{2}$$

 ©2003 The American Physical Society

where $k_{\pm}=k_x \pm i k_y$, $F=E_\nu^0+\Delta_1+\Delta_2+S_1+S_2+V$, $\lambda=E_\nu^0+S_1+V$, $G=E_\nu^0+\Delta_1-\Delta_2+S_1+S_2+V$, $S_1=D_1\varepsilon_{zz}+D_2(\varepsilon_{xx}+\varepsilon_{yy})$, $S_2=D_3\varepsilon_{zz}+D_4(\varepsilon_{xx}+\varepsilon_{yy})$, m_0 is the free electron mass, $P_1=-i(\hbar^2/m_0)\langle iS|\partial/\partial z|Z\rangle$, $P_2=-i(\hbar^2/m_0)\langle iS|\partial/\partial x|X\rangle=-i\hbar^2/m_0\langle iS|\partial/\partial x|Y\rangle$ are momentum matrix elements, E_c is the position of the Γ-point conduction band minimum, Δ_1 and $\Delta_{2,3}$ are parameters of the crystal field and spin-orbit interaction, respectively, E_ν^0 is the valence band edge position before the strain, crystal-field, and spin-orbit splittings are taken into account, D_i's are the deformation potentials, $\varepsilon_{xx}=\varepsilon_{yy}=(a_0-a)/a$, $\varepsilon_{zz}=-2C_{13}/C_{33}\varepsilon_{xx}$ are the strain components, C_{13} and C_{33} are the elastic coefficients, and a_0 and a are the lattice constants of the substrate and layer, respectively. We assume that z-dependent parameters E_c and E_ν^0 account for the heterostructure band offsets. Here V includes contributions from an external electric field (bias) and a self-consistent potential in an inhomogeneous structure. In Eq. (2), the shear strain components are neglected. Also, we keep only linear k terms in the off-diagonal matrix elements. The linear k approximation has also been used in spin splitting calculations in GaAs heterostructures.[13] As this approximation is valid if the typical electron energy is less than the band gap, it better describes the band spectrum in a wider band gap GaN.

The matrix Schrödinger equation for the eight-component envelope wave function has the form $H\varphi=\varepsilon\varphi$, where H is given in Eq. (2). In a heterostructure grown along the c axis (z direction), one has to replace k_z with $-i(\partial/\partial z)$ and keep band parameters z dependent. The system of eight equations can be exactly decoupled in to a two-component conduction band envelope function $\binom{\phi_1}{\phi_2}$ as

$$\begin{bmatrix} E_c+V+\dfrac{\hbar^2k_\parallel^2}{2m_\parallel}-\dfrac{\hbar^2}{2}\dfrac{\partial}{\partial z}\dfrac{1}{m_z}\dfrac{\partial}{\partial z}-\varepsilon & iP_1P_2k_-\dfrac{\partial\beta}{\partial z} \\ -iP_1P_2k_+\dfrac{\partial\beta}{\partial z} & E_c+V+\dfrac{\hbar^2k_\parallel^2}{2m_\parallel}-\dfrac{\hbar^2}{2}\dfrac{\partial}{\partial z}\dfrac{1}{m_z}\dfrac{\partial}{\partial z}-\varepsilon \end{bmatrix}\begin{pmatrix}\phi_1\\ \phi_2\end{pmatrix}=0, \tag{3}$$

where z dependent potential energy V accounts for the bias and electric field in the depletion regions and

$$m_\parallel^{-1}=\frac{1}{m_0}+\frac{2P_2^2}{\hbar^2}\frac{2\Delta_3^2-(\lambda-\varepsilon)(F+G-2\varepsilon)}{(F-\varepsilon)[(G-\varepsilon)(\lambda-\varepsilon)-2\Delta_3^2]},$$

$$m_z^{-1}=\frac{1}{m_0}+\frac{2P_1^2}{\hbar^2}\frac{(\varepsilon-G)}{(G-\varepsilon)(\lambda-\varepsilon)-2\Delta_3^2}, \tag{4}$$

$$\beta=\frac{\Delta_3}{(G-\varepsilon)(\lambda-\varepsilon)-2\Delta_3^2}.$$

In a relaxed GaN crystal the electron effective masses in Eq. (4) coincide with those obtained[32] assuming that the reference energy $E_\nu^0=0$, $\varepsilon\to E_c=E_g+\Delta_1+\Delta_2$, where E_g is the bandgap.

The diagonal part of the Hamiltonian in Eq. (3) has degenerate eigenfunctions $\Phi_1=\Phi_2=\Phi$. Nondiagonal terms in Eq. (3) lift the spin degeneracy. The energy difference between spin-up and spin-down conduction states (spin-splitting) can be written as

$$|\Delta\varepsilon|=2\alpha\sqrt{k_x^2+k_y^2},\quad \alpha=P_1P_2\left|\left\langle\frac{\partial\beta}{\partial z}\right\rangle\right|,\quad \langle f\rangle\equiv\int\Phi^*f\Phi dz. \tag{5}$$

Let us analyze the general expression for the spin-orbit splitting parameter α. In the $Al_xGa_{1-x}N/GaN/Al_yGa_{1-y}N$ QW of width L, the coefficient β can be represented as a sum of three terms each corresponding to a region i representing the left barrier L, the well W, and the right barrier R as follows:

$$\beta=\beta_L[1-\theta(z)]+\beta_W[\theta(z)-\theta(z-L)]+\beta_R\theta(z-L), \tag{6}$$

where $\theta(z)$ is the step function. The average over QW ground state follows from Eq. (6):

$$\left\langle\frac{\partial\beta}{\partial z}\right\rangle=\Phi^2(0)(\beta_W-\beta_L)-\Phi^2(L)(\beta_W-\beta_R)+q\langle B_LF_L\rangle+q\langle B_RF_R\rangle+q\langle B_WF_W\rangle, \tag{7}$$

where

$$\beta_i=\frac{\Delta_3}{(E_g+2\Delta_2-S_1-S_2+\varepsilon-V)(E_g+\Delta_1+\Delta_2-S_1+\varepsilon-V)-2\Delta_3^2},$$

$$B_i = \frac{\Delta_3[2E_g + \Delta_1 + 3\Delta_2 - 2S_1 - S_2 + 2(\varepsilon - V)]}{\{(E_g + 2\Delta_2 - S_1 - S_2 + \varepsilon - V)(E_g + \Delta_1 + \Delta_2 - S_1 + \varepsilon - V) - 2\Delta_3^2\}^2}, \tag{8}$$

$$F_i = \frac{1}{q}\frac{\partial V_i}{\partial z}.$$

The reference energy in Eq. (7) is the bottom of the conduction band. Each average value in Eq. (7) contains integration over the corresponding region i excluding interfaces located at $z=0$ and $z=L$. Potential jumps and offsets of band parameters at the interfaces contribute to the first two terms of Eq. (7). The energy parameter ε in all B_i and β_i should be taken at the ground electron level in the well, and $k_\parallel = 0$: $\varepsilon \to \varepsilon_1$. All other parameters in Eqs. (7) and (8) take the values attributed to the corresponding layer i.

If the barrier height tends to infinity, the coupling coefficient takes the form

$$\left\langle \frac{\partial \beta}{\partial z} \right\rangle = q\langle B_W F_W \rangle, \tag{9}$$

which is not exactly proportional to the average electric field in the well as long as B_W depends on z. Equation (7) gives no spin splitting in a symmetric QW where $\Phi^2(0)(\beta_W - \beta_{LB}) = \Phi^2(L)(\beta_W - \beta_{RB})$ and $\langle B_{LB}F_{LB}\rangle + \langle B_{RB}F_{RB}\rangle = \langle B_W F_W\rangle = 0$.

III. POLARIZATION-DOPED HETEROSTRUCTURE

In a HEMT structure, which comprises a AlGaN layer grown in the z direction on the top of a thick GaN layer, the spin-orbit coupling parameter (7) takes the form

$$\left\langle \frac{\partial \beta}{\partial z} \right\rangle = \Phi^2(0)(\beta_C - \beta_B) + q\langle B_B F_B\rangle + q\langle B_C F_C\rangle, \tag{10}$$

where B and C represent the AlGaN barrier and GaN channel, respectively.

We assume that the $Al_xGa_{1-x}N$ layer is grown on the top of a relaxed GaN with a Ga-polarity surface. In this case, the polarization field causes the conduction band to decrease in energy with decreasing distance toward the interface from both well and barrier sides as shown in Fig. 1.

The total polarization comprises two parts, namely, $P_{\text{tot}} = P_{\text{SP}} + P_{\text{PE}}$, where P_{SP} is the spontaneous polarization from both barrier and channel regions and P_{PE} is the piezoelectric polarization in the barrier caused by a lattice mismatch to GaN:

$$P_{\text{PE}} = e_{31}(\varepsilon_{xx} + \varepsilon_{yy}) + e_{33}\varepsilon_{zz},$$

$$P_{\text{SP}} = -0.052x - 0.029\left(\frac{C}{m^2}\right), \tag{11}$$

where e_{ij} are the piezoelectric coefficients in AlGaN.

Two-dimensional electrons confined in the GaN-channel partially compensate the total polarization charge P_{tot}. Uncompensated polarization charge creates the electric field across the barrier. Sheet electron density in the channel of the nominally undoped heterostructure is related to the Fermi level as[28]

$$n_S = \frac{P_{\text{tot}}}{q} - \frac{\varepsilon_B \varepsilon_0}{q^2 W_B}[\varphi_B - qV_g + E_F - \Delta E_C], \tag{12}$$

where φ_B is the height of the Schottky barrier on the top of the W_B-thick AlGaN layer, E_F is the Fermi energy, ΔE_C is the conduction band offset, and V_g is the gate voltage.

In the structure with the doped AlGaN barrier, the electron transfer from the barrier increases the total sheet electron density in the channel $N_c = n_S + N_D l$, which can be found from the equations[29]

$$\begin{cases} \Delta E_C - E_F - \varepsilon_d = \dfrac{q^2 N_D l^2}{2\varepsilon_0 \varepsilon_B}, \\ N_c = \dfrac{m_\parallel k_B T}{\pi \hbar^2} \ln\{1 + \exp[(E_F - \varepsilon_1)/k_B T]\}, \end{cases} \tag{13}$$

where $m_\parallel$ is the in-plane effective mass of channel electrons, N_D is the density of ionized donors in the l-thick space charge region on the AlGaN side of the structure, and ε_d is donor bound energy.

IV. ELECTRIC FIELDS AND WAVE FUNCTION

Electric fields across the channel F_C and the barrier F_B follow from the charge and electrostatic potential

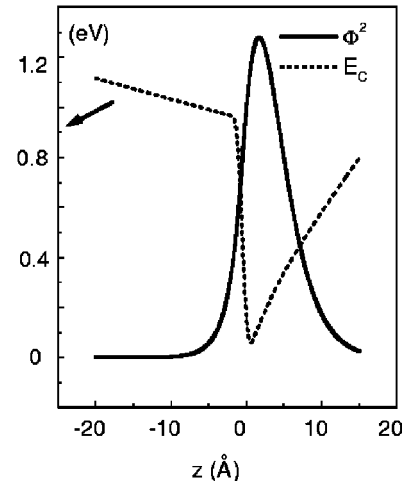

FIG. 1. Potential profile and wave function in $Al_{0.5}Ga_{0.5}N$/GaN heterostructure. Barrier thickness: 100 Å, barrier doping: $N_D = 10^{18}$ cm^{-3}. Interface is located at $z=0$.

balance.[24,28] The potential energy profile is shown in Fig. 1. The electric fields are given as

$$V_C = qF_C z,\quad F_C = \frac{qn_S}{\varepsilon_C \varepsilon_0},\quad z \geqslant 0,$$

$$V_B = \Delta E_C - qF_B z,\quad F_B = \frac{P_{\text{tot}} - qn_S}{\partial_C \varepsilon_0},\quad z < 0. \tag{14}$$

We will calculate the spin splitting of the ground state of 2D electrons in the channel neglecting higher subbands. Ground state wave function can be well represented by the Fang-Howard (FG) trial function.[33] Since wave function penetration into the barrier contributes to the spin-orbit coupling parameter of Eq. (10), we have to use the modified FG function that accounts for barrier penetration. Thus,

$$\Phi(z) = \begin{cases} Az_0 \sqrt{\frac{b^3}{2}} \exp(-\kappa_b z), & z \leqslant 0, \\ A(z+z_0)\sqrt{\frac{b^3}{2}} \exp(-bz/2), & z \geqslant 0, \quad \kappa_b = \sqrt{\frac{2m_{zB}\Delta E_C}{\hbar^2}} \end{cases}. \tag{15}$$

Parameters z_0 and A follow from normalization and matching condition for the electron flux through the interface

$$z_0 = \frac{2}{2\kappa_b m_{zC} m_{zB}^{-1} + b},\quad A^2 = \frac{4z_0^{-2}}{(2z_0^{-1}+b) + b^2 + b^3 \kappa_b^{-1}}, \tag{16}$$

where m_{zB}, m_{zC} are electron masses in the z direction in the barrier and well, respectively.

The total average energy E_{av} consists of three parts: the kinetic energy, the energy in the channel electric field, and the potential energy induced by other 2D electrons in the channel. It is written as

$$E_{\text{av}} = \langle T\rangle + \langle V_C\rangle + \frac{1}{2}\langle V_S\rangle, \tag{17}$$

where

$$\langle T\rangle = \left\langle -\frac{\hbar^2}{2m_{zC}}\frac{\partial^2}{\partial z^2}\right\rangle,\quad \langle V_C\rangle = qF_C\langle z\rangle,$$

$$\langle V_S\rangle = \frac{q^2 N_c}{\varepsilon\varepsilon_0}\left\langle z\int_z^\infty \Phi^2 dz' + \int_0^z z'\Phi^2 dz'\right\rangle. \tag{18}$$

The average electron energy in the well E_{av} is subject to minimization with respect to parameter b. Energy $\varepsilon_1 = \min(E_{\text{av}})$ is the ground state level in the 2D channel. Parameter $b_{\min}$ determines the spatial size of the wave function in the z direction.

Using Eqs. (12)–(18), one can find the wave function $\Phi(z)$, ground state energy ε_1, Fermi energy E_F, and total sheet density of electrons in the channel N_c self-consistently. After that, the electron spin-splitting at the Fermi level can be calculated with Eqs. (5) and (10).

TABLE I. Parameters of the $Al_xGa_{1-x}N$ material system.

Effective mass (m_0)	$0.22+0.26x$
Static dielectric constant (ε_0)	$10.4-0.3x$
Elastic constants (GPa)	$C_{13}=103+5x$; $C_{33}=405-32x$
Piezoelectric coefficients (C/m^2)	$e_{13}=-0.49-0.11x$; $e_{33}=0.73\,(1+x)$[a]
Schottky barrier height (eV)	$0.84+1.3x$[b]
Band gap (eV)	$3.4+2.7x$
Conduction band offset (eV)	$E_g(x)-E_g(0)-0.8x$
Lattice constant (Å)	$3.189-0.077x$
Donor ionization energy (meV)	38.0[c]
Spin-orbit split energy (meV),	$\Delta_2=\Delta_3=6.0$[d]
Crystal-field split energy (meV)	$\Delta_1=22.0-80.0x$[e]
Interband momentum-matrix elements $P_{1,2}=\hbar\sqrt{E_{1,2}/2m_0}$	$E_1=E_2=20.0$ eV

[a]Reference 25.
[b]Reference 34.
[c]Reference 35.
[d]Reference 36.
[e]Reference 32.

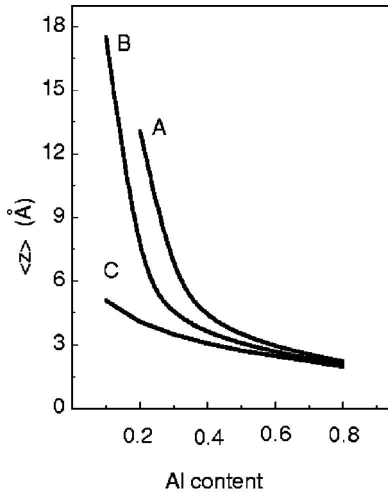

FIG. 2. Width of the electron channel near GaN/AlGaN interface for various values of gate voltages. Lines A, B, and C correspond to gate voltages $V_g=(-0.8,0,0.8)$ V, respectively.

V. RESULTS AND DISCUSSION

In this section we calculate the spin-splitting of channel electrons in GaN-based field effect transistor and compare it with the magnitude of Rashba effect in Ga(In,Al)As materials. Material parameters used in numerical calculations are given in Table I.

The conduction band offset, shown in Table I, is calculated using the linear alloy approximation for the valence band offset [0.8 eV between GaN and AlN (Ref. 37)]. To estimate spin splitting up to a high Al content in the barrier, we choose a barrier thickness of 100 Å. We assume this thickness is less than the critical thickness of the AlGaN layer up to $x=0.8$. This assumption allows using the piezoelectric polarization Eq. (11) for the pseudomorphic layer without having to include a partial stress relaxation, which otherwise should be taken into account for thicker layers.[30] Calculations below were done with the barrier doping $N_D=10^{18}$ cm^{-3}.

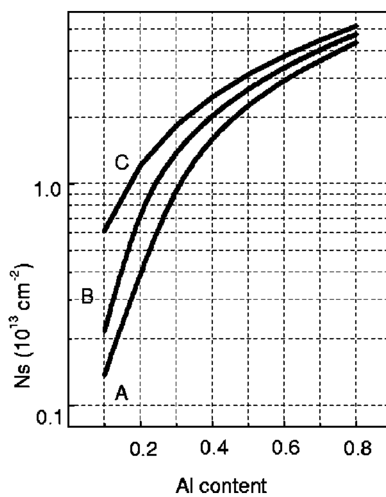

FIG. 3. Total sheet carrier concentration in the channel with different gate voltages. Lines A, B, and C correspond to gate voltages $V_g=-0.8$, 0, 0.8 (V), respectively.

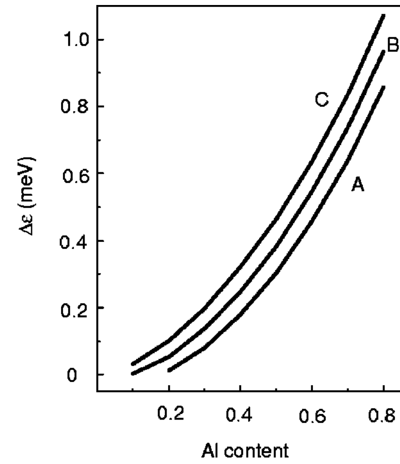

FIG. 4. Electron spin-splitting energy. Barrier thickness 100 Å, barrier doping $N_D=10^{18}$ cm^{-3}. Lines A, B, and C correspond to gate voltages $V_g=-0.8$, 0, 0.8 (V), respectively.

The wave function for the particular choice of parameters is illustrated in Fig. 1. Effective thickness of the bound sheet electrons near an interface is given as $d=\int_0^\infty z\Phi^2(z)dz$ and shown in Fig. 2 as a function of Al content in the barrier.

Figure 2 illustrates the gate-controlled effective distance of the 2D gas from the interface. The distance, in turn, could control kinetic characteristics of electrons: large distance makes higher the electron mobility with respect to scattering on interface roughness and interface-induced structural defects. The total sheet electron concentration as a function of Al composition and gate voltage is given in Fig. 3.

Gate-controlled carrier density in the channel is shown in Fig. 3. The lower the Al content in the barrier material the higher sensitivity of the carrier density to an external bias. At $V_g=0$ the result is quite close to that obtained in Ref. 30.

The built-in electric field in the channel F_C calculated at $x=0.2(1.1$ MV/cm) and $x=0.5(4.2$ MV/cm) are in a good agreement with those typically observed in GaN/AlGaN QW.[38]

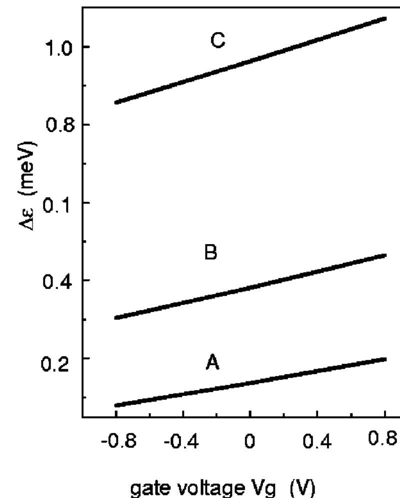

FIG. 5. Electron spin-splitting in the channel under the gate bias. Lines A, B, and C correspond to alloy compositions $x=0.3$, 0.5, 0.8, respectively.

The electron spin splitting $|\Delta\varepsilon|$, calculated at the Fermi level as a function of Al content in the barrier is given in Fig. 4, and as a function of gate voltage in Fig. 5.

As seen in Figs. 4 and 5, the spin splitting is gate voltage tunable and of the same order of magnitude as in other group-III-V materials: in InAlAs/InGaAs QW, it approximately equals 1.0 meV.[39] More complete information about spin-splitting in narrow-gap materials can be found in Ref. 18, which lists spin-splitting magnitude across all group-III-V nanostructures between 1 to 10 meV. Electron spin splitting, governed by a gate voltage, is at heart of the spin-transistor proposal.[6] Gate-controlled spin-splitting allows fitting the phase difference of spin-up and spin-down electron wave functions, acquired on the channel length. Since the drain current oscillates with the phase difference, one could punch-off the channel varying the electron phase. This is much less power consuming and much faster process than pushing electrons in and out of the channel in field-effect transistors. The results, shown in Figs. 4 and 5, give a quantitative sense of the magnitude of the Rashba effect in GaN-based materials.

In conclusion, in spite of the large bandgap in GaN-based heterostructures, electron spin splitting is predicted to be comparable to that in Ga(In, Al)As materials due to a strong polarization doping effect in the GaN/AlGaN heterostructure. It is also worth noting that GaN layers being doped with transition metal impurities reveal room temperature ferromagnetism, thus making possible lattice-matched all-semiconductor spin-transistor structures, which are supposed to provide effective spin injection in the channel. The main point of this paper is to attract attention to the GaN material system in terms of its potential importance in various spintronic applications.

---

*Electronic address: vlitvinov@waveband.com

[1] S. A. Wolf, D. D. Awschalom, R. A. Buhrman, J. M. Daughton, S. von Molnar, M. L. Roukes, A. Y. Chtchelkanova, and D. M. Treger, Science **294**, 1488 (2001).

[2] J. M. Kikkawa and D. D. Awschalom, Phys. Rev. Lett. **80**, 4313 (1998).

[3] F. Matsukura, H. Ohno, A. Shen, and Y. Sugawara, Phys. Rev. B **57**, R2037 (1998).

[4] B. Beschoten, P. A. Crowell, I. Malajovich, D. D. Awschalom, F. Matsukura, A. Shen, and H. Ohno, Phys. Rev. Lett. **83**, 3073 (1999).

[5] K. W. Edmonds, K. Y. Wang, R. P. Campion, A. C. Neumann, N. R. S. Farley, B. L. Gallagher, and C. T. Foxon, Appl. Phys. Lett. **81**, 4991 (2002).

[6] S. Datta and B. Das, Appl. Phys. Lett. **56**, 665 (1989).

[7] J. Nitta, T. Akazaki, H. Takayanagi, and T. Enoki, Phys. Rev. Lett. **78**, 1335 (1997).

[8] S. Bandyopadhyay, Phys. Rev. B **61**, 13 813 (2000).

[9] G. Dresselhaus, Phys. Rev. **100**, 580 (1955).

[10] E. I. Rashba and V. I. Sheka, Fiz. Tverd. Tela (Leningrad) **3**, 1735 (1961) [Sov. Phys. Solid State **3**, 1257 (1961)].

[11] E. I. Rashba, Fiz. Tverd. Tela (Leningrad) **2**, 1224 (1960) [Sov. Phys. Solid State **2**, 1109 (1960)]; Yu. A. Bychkov and E. I. Rashba, J. Phys. C **17**, 6039 (1984).

[12] F. T. Vas'ko, JETP Lett. **30**, 541 (1979).

[13] L. G. Gerchikov and A. V. Subashiev, Sov. Phys. Semicond. **26**, 73 (1992).

[14] E. A. de Andrada e Silva, G. C. La Rocca, and F. Bassani, Phys. Rev. B **50**, 8523 (1994); **55**, 16 293 (1997).

[15] P. Pfeffer and W. Zawadzki, Phys. Rev. B **59**, R5312 (1999).

[16] G. Engels, J. Lange, and H. Luth, Phys. Rev. B **55**, R1958 (1997); Th. Schäpers, G. Engels, J. Lange, Th. Klocke, M. Hollfelder, and H. Luth, J. Appl. Phys. **83**, 4324 (1998).

[17] P. Pfeffer and W. Zawadzki, Phys. Rev. B **52**, R14 332 (1995).

[18] D. D. Awshalom, D. Loss, and N. Samarth, *Semiconductor Spintronics and Quantum Computation* (Springer, Berlin, 2002).

[19] T. Dietl, H. Ohno, F. Matsukara, J. Cibert, and D. Ferrand, Science **287**, 1019 (2000).

[20] V. I. Litvinov and V. K. Dugaev, Phys. Rev. Lett. **86**, 5593 (2001).

[21] S. Sonoda, S. Shimizu, T. Sasaki, Y. Yamamoto, and H. Hori, cond-mat/0108159 (unpublished).

[22] M. L. Reed, N. A. El-Mastry, H. H. Stadelmaier, M. K. Riturns, M. J. Reed, C. A. Parker, J. C. Roberts, and S. M. Bedair, Appl. Phys. Lett. **79**, 3473 (2001).

[23] S. G. Yang, A. B. Pakhomov, S. T. Hung, and C. Y. Wong, Appl. Phys. Lett. **81**, 2418 (2002).

[24] A. Bykhovsky, B. Gelmont, and M. Shur, J. Appl. Phys. **74**, 6734 (1993).

[25] F. Bernardini, V. Fiorentini, and D. Vanderbilt, Phys. Rev. B **56**, R10 024 (1997); Phys. Rev. Lett. **79**, 3958 (1997).

[26] R. Cingolani, A. Botchkarev, H. Tang, H. Morkoc, G. Traetta, G. Golli, M. Lomascolo, A. Di Carlo, F. Della Sala, and P. Lugli, Phys. Rev. B **61**, 2711 (2000).

[27] M. S. Shur, A. D. Bykhovsky, and R. Gaska, MRS Internet J. Nitride Semicond. Res. **4S1**, G1.6 (1999).

[28] E. T. Yu, G. J. Sullivan, P. M. Asbeck, C. D. Wang, D. Qiao, and S. S. Lau, Appl. Phys. Lett. **71**, 2794 (1997).

[29] T. H. Yu and K. Brennan, J. Appl. Phys. **89**, 3827 (2001).

[30] O. Ambacher, B. Foutz, J. Smart, J. R. Shealy, N. G. Weimann, K. Chu, M. Murphy, A. J. Sierakowski, W. J. Shaff, L. F. Eastman, R. Dimitrov, A. Mitchell, and M. Stutzmann, J. Appl. Phys. **87**, 334 (2000).

[31] G. L. Bir and G. E. Pikus, *Symmetry and Strain Effects in Semiconductors* (Wiley, New York, 1974).

[32] S. Chuang and C. S. Chang, Phys. Rev. B **54**, 2491 (1996).

[33] T. Ando, A. B. Fowler, and F. Stern, Rev. Mod. Phys. **54**, 437 (1982); G. Bastard, *Wave Mechanics Applied to Semiconductor Heterostructures* (Halsted, Paris, 1988).

[34] L. S. Yu, D. J. Qiao, Q. J. Xing, S. S. Lau, K. S. Boutros, and J. M. Redwing, Appl. Phys. Lett. **73**, 238 (1998).

[35] H. Wang and A. B. Chen, J. Appl. Phys. **87**, 7859 (2000).

[36] M. Suzuki, T. Uenomyama, and A. Yanase, Phys. Rev. B **52**, 8132 (1995).

[37] S. H. Wei and A. Zunger, Appl. Phys. Lett. **72**, 2011 (1998).

[38] H. M. Ng, R. Harrel, S. N. G. Chu, and A. Y. Cho, J. Electron. Mater. **30**, 134 (2001).

[39] T. Koga, J. Nitta, T. Akazaki, and H. Takayanagi, Phys. Rev. Lett. **89**, 046801 (2002).